Stochastic Simulation and Performance Analysis of Classical Knock Control Algorithms

James C. Peyton Jones*, Jesse Frey‡,
Electrical and Computer Engineering*, Mathematics and Statistics‡
Center for Nonlinear Dynamics and Control, Villanova University, USA

Abstract
New methods are developed for predicting and quantifying the closed-loop performance of a standard advance-retard knock control algorithm, based on a computationally efficient Markov or first-step analysis. The results provide new insight into the steady-state and transient response of the controller and enable these characteristics to be quantified in a more rigorous and repeatable way than has previously been possible.

1. Introduction

Although there is a large and rich literature on knock sensing and detection [XX-XX], there has been relatively little work directly in the field of knock control. Notable exceptions include works by XX, XX, XX, [XX-XX], as well as recent work by the authors, [XX-XX], but the large majority of production knock controllers still employ a 'conventional' advance-retard type knock control strategy whose form has not changed in many years. Given the maturity of this strategy, it is quite surprising that there exists no rigorous analysis of its performance. Typical studies present a time history trace of the closed loop spark advance, but it is hard to assess performance relative to the target knock rate or knock probability objective. Furthermore, a single time history represents the response to one instance of the knock process. Since knock events occur randomly, re-running the experiment or simulation will likely yield a different result, making it hard to obtain any rigorous or repeatable performance metrics.

To address this issue, the authors recently proposed a stochastic simulation method which yields not just a specific time history trace, but rather the time history of the closed-loop spark advance or knock probability *distribution*, including both transient and steady state distributions [XX]. It was also shown how the mean and $5^{th}/95^{th}$ percentile response curves to all possible knock instances resulting from some initial condition could be evaluated, providing a much deeper insight into closed loop behavior. In this paper, the same approach is extended in order to compute a variety of performance metrics. Section 2 describes the operation of the conventional control strategy, including such details as limited spark angle resolution, and a typical closed-loop simulation of such a system is presented. The more general stochastic simulation methodology is introduced in Section 3, showing how it is possible to compute the distribution of the closed-loop spark advance, or instantaneous closed-loop knock probability as a function of cycle number, n. It is also straightforward to quantify the steady state spark or knock probability distributions which define the steady-state controller performance. The transient performance of the controller is addressed in Section 4, where a variety of metrics are developed in order to predict and quantify the speed of response, or the number of knock events that occur during the transient period. Together, these tools provide a much more rigorous and complete assessment of closed-loop knock controller performance than has previously been possible.

2. Conventional Knock Control

Although the feedback sensor and initial knock signal processing varies considerably from one system to the next, almost all knock controllers apply a threshold to the resulting knock intensity metric (however obtained) in order to generate knock events which are fed back to the controller. Typically the threshold is set at a level that identifies potentially damaging knock events, and the control objective is then to regulate these knock events to a low, (typically 1%), rate. This rate is strongly dependent on the spark advance, which is used as the manipulated variable for the controller. Although the knock probability characteristic varies with engine operating condition, a typical curve, taken at 1000 rpm from a XX Ford V6 engine, is shown in Fig. 1 (smooth curve), [XX]. Spark advance is shown relative to the Borderline (BL) audible knock condition, as identified by an expert calibration engineer, and the knock threshold is adjusted such that the target knock rate occurs at this condition. If the spark is advanced relative to BL, the knock rate increases rapidly. If it is retarded, the knock rate decreases only slightly, but fuel economy decreases also. An ideal knock controller would therefore use the knock event feedback signal in order to adjust the spark so as to operate as closely as possible to the 1% knock rate BL condition, rapidly returning to this condition when perturbed by any disturbances.

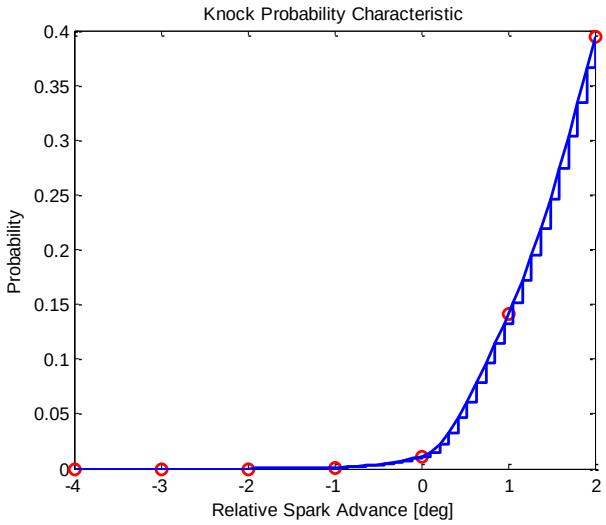

Fig. 1: Knock probability characteristic

Conventional knock control strategies essentially seek the knock limit by advancing the spark angle by a small amount K_{adv} every cycle until a knock event occurs, at which point the spark is rapidly retarded by a much larger amount K_{ret} in order to return the engine quickly to a safe operating condition. The control strategy can therefore be expressed as,

$$\theta(n+1) = \begin{cases} \theta(n) - K_{ret} & \textit{if knocking} \\ \theta(n) + K_{adv} & \textit{otherwise} \end{cases} \tag{1}$$

where $\theta(n)$ represents the spark angle at cycle n relative to the spark angle at borderline knock. Assuming stable control about some mean spark advance θ^*, retard events which occur with probability p^*, must on average cancel advance increments which occur with probability $(1 - p^*)$. The steady state closed loop knock probability can therefore be found according to,

$$K_{ret}\, p^* = K_{adv}(1-p^*) \quad => \quad p^* = \frac{K_{adv}}{K_{ret}+K_{adv}} \tag{2}$$

The closed loop knock probability is therefore easily defined by appropriate choice of the controller gains.

The control law is also sometimes expressed as,

$$\theta(n+1) = \theta(n) + K_{adv} - k\,K'_{ret} \quad \text{where} \quad k = \begin{cases} 1 & \textit{if knocking} \\ 0 & \textit{otherwise} \end{cases} \tag{3}$$

Note, in this formulation, that K_{adv} occurs on every cycle, so the actual total retard when knock occurs is $K_{ret} = (K'_{ret} - K_{adv})$. With this definition, the two expressions (1), (3), are identical, although the advantage of (3) is that the expressions relating the controller gains to knock probability are slightly simpler:

$$p^* = \frac{K_{adv}}{K'_{ret}} \tag{4}$$

The basic operation of the algorithm is very straightforward, but some minor practical details are worthy of discussion. The states θ_i of the controller, for example, are generally limited to a discrete and finite set,

$$\boldsymbol{\theta} = \{\theta_1, ..., \theta_{i_{\max}}\} \quad \text{where} \quad \theta_i = \theta_{\min} + (i-1)\Delta \tag{5}$$

due to the angular resolution Δ of the commanded spark advance. The quantities $\theta_{\min}$, $\theta_{\max}$ denote minimum and maximum limits placed on the spark advance, and the maximum index, $i_{\max}$ is given by $i_{\max} = ((\theta_{\max} - \theta_{\min})/\Delta) + 1$. The controller gains are chosen as integer multiples of Δ, such that,

$$\begin{aligned} K_{adv} &= m_1\Delta \\ K_{ret} &= m_2\Delta \end{aligned} \quad \Rightarrow \quad p^* = \frac{m_1}{m_1+m_2} \tag{6}$$

The control law is then also easy to implement using the index arithmetic as,

$$i_{n+1} = \begin{cases} i_n - m'_2 & \textit{if knocking} \quad m'_2 = \min(m_2, i_n - 1) \\ i_n + m'_1 & \textit{otherwise} \quad m'_1 = \min(m_1, [i_{\max} - i_n]) \end{cases} \tag{7}$$

where this form also includes the upper and lower saturation limits placed on the spark advance. Note, also, that the angular resolution Δ of the control algorithm is often significantly smaller than the resolution δ of spark angle actuation that can be implemented by the ECU. The actual spark angle θ' experienced by the engine is therefore given by,

$$\theta' = \textit{floor}(\theta, \delta) \tag{8}$$

where the function *floor* is used to indicate rounding downwards towards the nearest integer multiple of δ. This also means that the actual knock probability $p'(\theta)$ experienced by the engine, is

$$p'(\theta) = p(\theta') \tag{9}$$

A plot of the knock probability characteristic of the engine, discretized in this way, is shown in Fig. 1 (stepped curve). Typical time-history traces of the closed loop response to different initial conditions are also shown in Fig. 2, for p=0.01, and K'_{ret} = 1.5°, (hence K_{adv} = 0.015°). The algorithm resolution was set to be Δ = 0.015 degrees, so in this case m_1=1 and m_2= 100, and the ECU spark advance actuation resolution was assumed to be 0.1 degree. The effect of the limited ECU resolution can be seen in the fine staircase-like increments in spark advance, but otherwise the traces exhibit the classic sawtooth-like response, with sharp decrements whenever knock events occur.

Although these responses are indicative of system behavior, a different sequence of knock events will result in result in a different response trace, making it hard to quantify the performance of the controller in any repeatable way. In the following section, new methods are developed for predicting and quantifying the speed of the response and the steady state performance of the controller in a rigorous stochastic framework. The example system, whose response is shown in Fig. 2, will be used as a reference case to illustrate the results.

Figure needs inserting

Fig. 2:

3. Stochastic Simulation

In contrast to the specific time history simulations of Fig. 2, a stochastic simulation propagates some initial probability distribution of the controller state $P_0(\theta_i)$ forward in time using the control law (7), and the knock probability characteristic of the engine, Fig. 1. This evolution may be defined recursively according to,

$$P_{n+1}(\theta_0) = \sum_{j=0}^{m_2} p'(\theta_j)\ P_n(\theta_j) \tag{10}$$

$$P_{n+1}(\theta_i) = \left(1 - p'(\theta_{i-m_1})\right)\ P_n(\theta_{i-m_1}) \ +\ p'(\theta_{i+m_2})\ P_n(\theta_{i+m_2}) \ , \qquad 0 < i < i_{\max} \tag{11}$$

$$P_{n+1}(\theta_{i_{\max}}) = \sum_{j=0}^{m_1} \left(1 - p'(\theta_{i_{\max}-j})\right) P_n(\theta_{i_{\max}-j}) \tag{12}$$

where $P_n(\theta_i)$, denotes the probability of being in state θ_i at cycle number n, and where $P_n(\theta_i)$=0 outside the limits $0 < i < i_{max}$. These expressions were derived in [XX], and are simply restated here, with the addition of some minor improvements in subscript notation, and the use of the discretized probability characteristic $p'(\theta)$ in place of the continuous characteristic $p(\theta)$. Of the three equations, equation (11) represents the most common case in which the probability, $P_n(\theta_i)$, has only two contributing terms – the first representing the probability of advancing into state θ_i from state $\theta_{i\text{-}m_1}$ due to a non-knocking cycle, and the second term representing the probability of retarding into state θ_i from state θ_{i+m2} as the result of a knock event. The other equations (10), (12), define the special cases that arise from saturation of the controller output at the limits $\theta_{\min}$, $\theta_{\max}$, respectively.

The three relations (10)-(12), can be written in the matrix form,

$$\mathbf{P}_{n+1}(\boldsymbol{\theta}) = \mathbf{M}^T \mathbf{P}_n(\boldsymbol{\theta}) \tag{13}$$

where $\mathbf{P}_n(\boldsymbol{\theta})$ is a column vector whose ith element is $P_n(\theta_i)$, and where the transition matrix $\mathbf{M}$ is a sparse, partially band diagonal matrix whose non-zero elements are defined according to,

$$\left.\begin{aligned} \mathbf{M}^{ret}_{i,i-m_2'} &= p(\theta_i) \qquad \forall\ i \mid (1 \le i \le i_{\max}) \\ \mathbf{M}^{adv}_{i,i+m_1'} &= \left(1 - p(\theta_i)\right) \quad \forall\ i \mid (1 \le i \le i_{\max}) \end{aligned}\right\} \quad \mathbf{M} = \mathbf{M}^{ret} + \mathbf{M}^{adv} \tag{14}$$

The matrix $\mathbf{M}$ therefore has the form,

$$\mathbf{M} = \begin{bmatrix} p'(\theta_0) & 0 & \left(1-p'(\theta_0)\right) & 0 & 0 & 0 & 0 \\ \vdots & 0 & 0 & \left(1-p'(\theta_1)\right) & 0 & 0 & 0 \\ p'(\theta_{m_2}) & 0 & 0 & 0 & \ddots & 0 & 0 \\ 0 & p'(\theta_{m_2+1}) & 0 & 0 & 0 & \ddots & 0 \\ 0 & 0 & \ddots & 0 & 0 & 0 & \left(1-p'(\theta_{i_{\max}-m_1})\right) \\ 0 & 0 & 0 & \ddots & 0 & 0 & \vdots \\ 0 & 0 & 0 & 0 & p'(\theta_{i_{\max}}) & 0 & \left(1-p'(\theta_{i_{\max}})\right) \end{bmatrix} \begin{matrix} \\ \\ \\ \\ \\ \\ \\ \end{matrix} \begin{matrix} \\ \updownarrow m_2 \\ \\ \\ \\ \\ \updownarrow m_1 \end{matrix} \tag{15}$$

The distribution of the closed loop spark advance at any cycle n, in response to an initial distribution specified in $\mathbf{P}_0(\boldsymbol{\theta})$, is then computed by repeated application of (13) giving,

$$\mathbf{P}_n(\boldsymbol{\theta}) = \left(\mathbf{M}^T\right)^n \mathbf{P}_0(\boldsymbol{\theta}) \qquad n \ge 0 \tag{16}$$

Furthermore the steady state distribution is readily obtained as the probability vector solution to,

$$(\mathbf{M}^T - \mathbf{I})\ \mathbf{P}_\infty(\boldsymbol{\theta}) = 0 \tag{17}$$

The steady state distribution for the system described in Section 2, for example, is shown in Fig. 3, and it is a simple matter to compute the mean and standard deviation of the distribution as annotated in the figure. Note that the mean is slightly retarded with respect to the desired BL condition. This is due to the relatively broad distribution coupled with the asymmetric nature of the knock probability curve (Fig. 1) which requires a large number of cycles to operate at low knock probability in order to compensate for the upper tail of the distribution where the knock probability is much higher. Dispersion in closed loop spark advance is therefore closely related to degradation in mean spark timing and engine efficiency, and the relatively broad dispersion observed in Fig. 3 is an undesirable characteristic of the classical knock control algorithm.

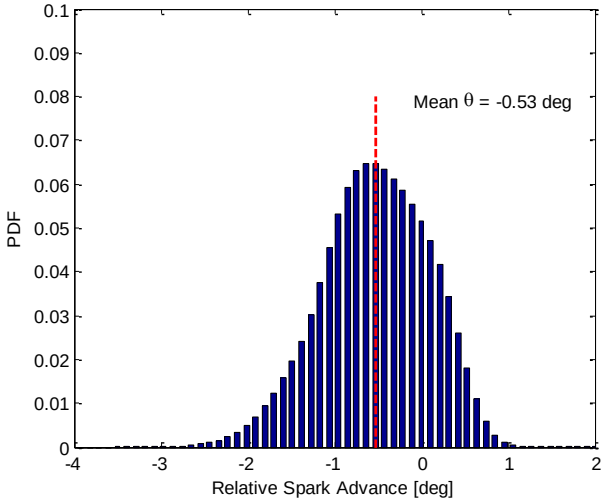

Fig. 3: Steady state distribution of the closed loop spark advance

The spark advance distribution is of interest from the perspective of engine efficiency. From a knock control perspective, however, it is useful to compute the distribution of the instantaneous knock rate, $P_n(p_i)$. This is readily achieved by mapping the spark advance distributions to knock probability distributions according to the knock probability characteristic defined by Fig. 1,

$$P_n(p_i) = P_n(\theta_i) \quad \text{where } p_i = p(\theta_i) \tag{18}$$

The resulting steady state knock probability distribution is shown in Fig. 4. Note that the mean knock rate is 0.01 as expected, but the distribution is highly skewed. As discussed above, this skew is caused by the upper tail of the spark angle distribution, amplified by the knock characteristic of Fig. 1, which causes a few cycles to operate at very high knock rates. To compensate, many cycles must operate below the target knock rate, resulting in a highly asymmetric distribution. From a practical perspective, this means that many cycles operate with sub-optimal efficiency, while a few cycles operate with significant knock risk.

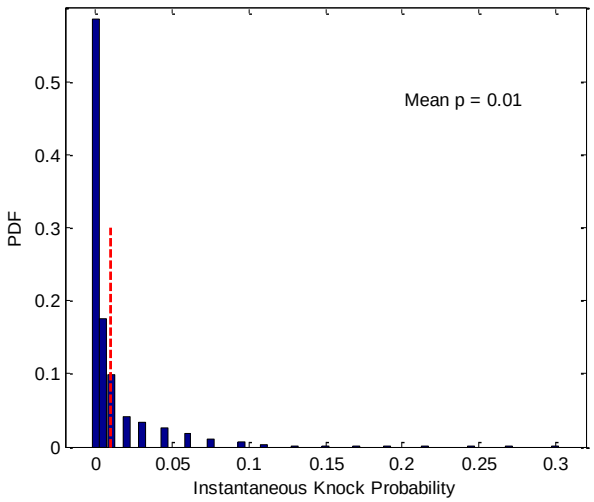

Fig. 4: Steady state distribution of the closed loop instantaneous knock probability

The spark advance and knock probability distributions of Figs. 3, 4, provide a useful measure of steady state performance, but it is important to note that the distribution at some finite cycle number n does not converge to the steady state distribution quickly. Instead, it remains concentrated in a small number of discrete states for quite some time. Using (16), for example, the distribution for n= 230, is shown in Fig. 5, which bears little resemblance to Fig. 3. Indeed, an intensity plot of the PDF amplitude as a function of cycle number and spark advance (Fig. 6), shows a periodic pattern shifting 'upward' with each cycle, where the distribution at any given cycle number (such as n= 230, illustrated by the dashed line in Fig. 6), gives a discrete distribution as illustrated in Fig. 5.

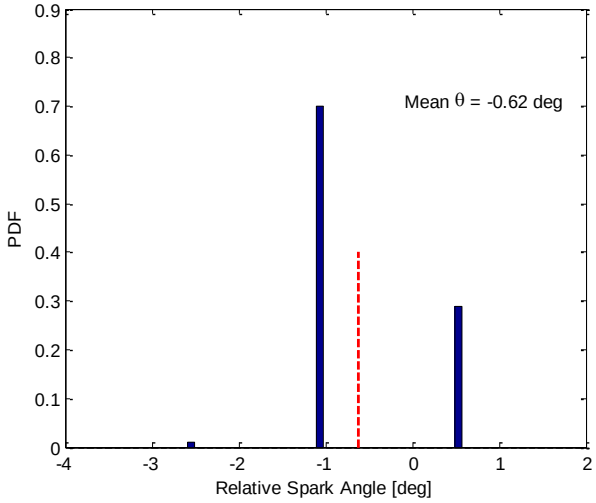

Fig. 5: Distribution of the closed loop spark advance at cycle number n = 230.

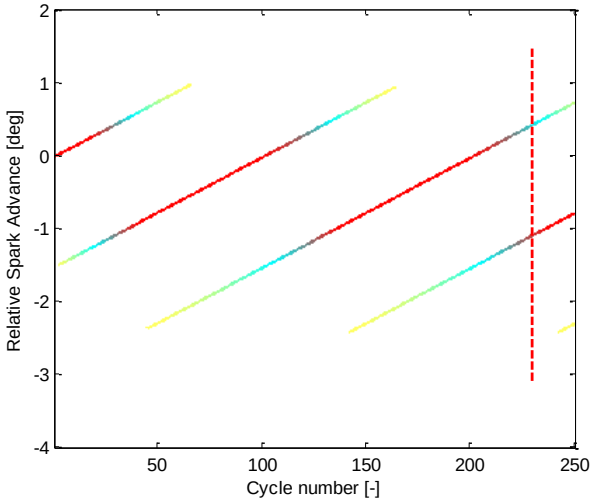

Fig. 6: Intensity plot of the distribution of the closed loop spark advance

This behavior is a direct result of the control law which employs fixed amplitude control moves K_{ret}, K_{adv}, except in the (usually rare) cases where the upper or lower saturation limits are encountered. In the absence of these limits, an expression for the controller index i_n at cycle number n, after k knock events and (n-k) non-knock events, is given by,

$$i_n = i_o + (n-k)m_1 - k\,m_2 = i_o + (np^* - k)(m_1 + m_2) \tag{19}$$

where the second equality follows from (6), and where the factor (np^*- k) in the second term can be recognized as the excess or deficiency of knock events relative to the target knock rate. Inspection of (19) shows that for fixed k, the index i_n is a linear function of cycle number n, with gradient m_1, as indeed observed in Fig. 6. Similarly, for any given value of n, the only variable in (19) is the number of knock events k, and any increment or decrement of this number shifts the output index i_n by an amount (m_1+m_2). The output spark angle therefore falls, as observed in Fig. 5 and 6, into discrete states separated by an angular distance K_{adv}+K_{ret}. Finally, the period, T, of this cyclic behavior can be obtained by equating points i_n and i_{n+T} where the latter is 'separated' from the former not only by the period T, but also by the occurrence of one additional knock event. This yields,

$$(n+T)p^* - (k+1) = np^* - k \qquad \Rightarrow \qquad T = 1/p^* \tag{20}$$

The period in this case, where p^* = 0.01, is therefore 100 cycles, as indeed observed in Fig. 6. This pattern only breaks down when, with small but finite probability, the upper or lower saturation limits are encountered. The expression (19) then no longer holds since the variables m_1, m_2 should be replaced by their limited counterparts, m_1', m_2', and some spread in the distribution begins to occur, finally evolving to the steady state distribution seen in Fig. 3.

Given the non-stationary nature of the response observed in Fig. 6, it is important to distinguish between sample and ensemble distributions. The two are identical in the limit as n tends to infinity, but for smaller values of n there are significant differences. In such cases, the sample or time-averaged distribution $\bar{P}_n(\theta_i)$ is arguably more representative of the response over the relatively short periods that may occur before the engine moves to a different operating point. It is also easier to estimate experimentally as,

$$\bar{P}_n(\theta_i) = \frac{c_i}{n} = \frac{1}{n}\sum_{j=1}^{n} I\left(\theta(j) = \theta_i\right) \qquad \forall\ \theta_i \in \boldsymbol{\theta} \tag{21}$$

where $I(A)$ is the indicator function of an event A, and c_i is the observed count of spark advance angles equal to θ_i in the sample $\{\theta(1),\ldots,\theta(n)\}$. The expected sample distribution, $\bar{\mathbf{P}}_n(\boldsymbol{\theta})$, can also be computed theoretically according to,

$$\bar{\mathbf{P}}_n(\boldsymbol{\theta}) = \frac{1}{n}\sum_{j=1}^{n} \mathbf{P}_j(\boldsymbol{\theta}) \tag{22}$$

where $\mathbf{P}_j(\boldsymbol{\theta})$ is given by (13). Fig. 7, for example, presents the expected sample distribution for the example system over the first n= 230 cycles. Note that the result is very different from the ensemble distribution at the specific cycle n= 230, shown in Fig. 5, and is much closer to the steady state ensemble distribution, Fig. 3. Indeed, the time averaged distribution converges much more rapidly to the steady state ensemble distribution than does $P_n(\theta_i)$ itself.

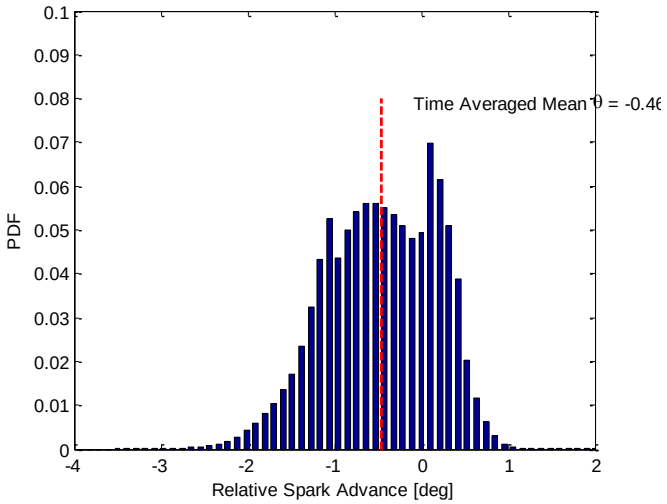

Fig. 7: Time-averaged distribution of the closed loop spark advance at n=230 cycles

4. Quantifying the transient response

The closed loop steady state or time-averaged distributions shown in Figs. 3,4,7 provide a useful measure of the steady state or averaged controller error, but the transient response of the controller is also critical in order to guarantee quick recovery from knocking conditions, or from overly retarded conditions. This transient response is most completely characterized by the time evolution of the ensemble distribution, computed according to (13), where the initial condition represents some sudden disturbance experienced by the engine. However, the multi-dimensional nature of this response makes it hard to visualize or compare quantitatively. In this section, a variety of statistical measures are therefore developed to reduce the dimensionality and to provide quantitative metrics for the transient performance of the controller.

4.1 *Finding the ensemble mean spark advance and knock probability transient response.*

Computation of the mean spark advance and mean knock probability response has been previously presented [XX], but the results are briefly repeated here for the sake of completeness. The time history of the mean spark advance, $\mu_\theta(n,\theta_0)$, starting from some initial disturbance condition θ_0, is easily computed from the time history of the ensemble distribution $P_n(\theta_i)$,

$$\mu_\theta(n,\theta_0) = \sum_{i=0}^{i_{\max}} P_n(\theta_i)\,\theta_i = \boldsymbol{\theta}^T\,\mathbf{P}_n(\boldsymbol{\theta}) \tag{23}$$

Fig. 8, for example, shows the mean closed loop spark angle response for a variety of initial conditions including the three initial conditions considered in the instance-specific simulations of Fig. 2. The somewhat jagged nature of the responses is due to the limited actuator resolution, but the underlying curves show a smooth transition from the initial condition to a limit-cycle-like oscillation about a slightly retarded mean value of -0.53°. These oscillations reflect the periodic nature of the spark advance distribution discussed in the previous section, and will eventually decay to the mean of the steady state distribution, (Fig. 3). The speed of the initial transient, however, depends very much on the initial condition. When initialized with the BL+1.6° advance, for example, the controller rapidly retards the spark and quickly enters the limit cycle

state. When initialized in a more retarded condition, eg. BL-1.6°, the recovery is much slower due to the relatively small magnitude of the advance gain K_{adv}.

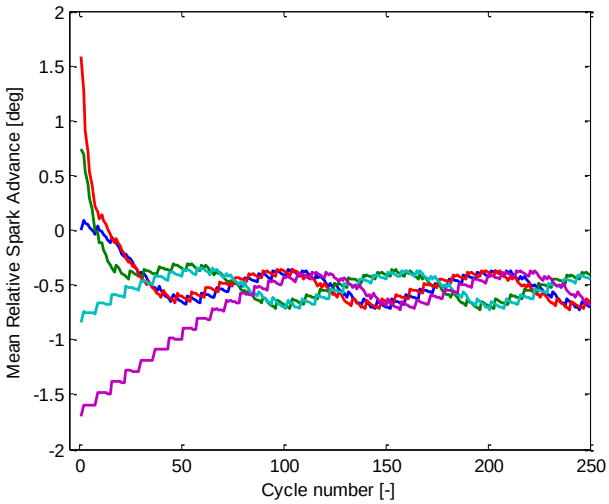

Fig. 8: Transient response of the ensemble mean spark advance from different initial conditions.

The mean instantaneous knock probability, $\mu_p(n,\theta_0)$ is also easily computed using the mapping (18) and the standard expression,

$$\mu_p(n,\theta_0) = \sum_{i=1}^{i_{\max}} P_n(\theta_i)\ p_i = \mathbf{p}^T \mathbf{P}_n(\boldsymbol{\theta}) \tag{24}$$

The results, for the same initial conditions considered in Fig. 8, are presented in Fig. 9. As expected, the mean knock probability curves have similar characteristics to those for the mean spark curves, in terms of the speed of response and limit-cycle-like behavior. In this case, however, it is easier to be quantitative about the performance relative to the 1% knock probability target, and the mean instantaneous knock probability is seen to oscillate in the 0.5 - 2.0% range.

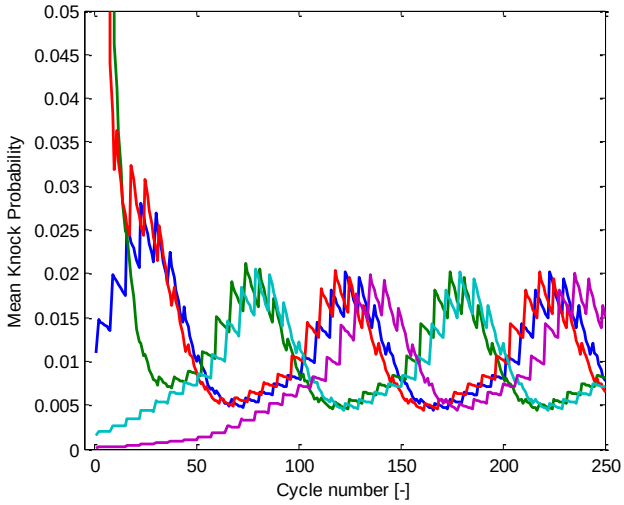

Fig. 9: Transient response of the mean knock probability from different initial conditions.

4.2 *Finding the mean time-averaged spark advance transient response time.*
As well as computing the ensemble characteristics of the closed loop response, the mean sample- or time-averaged response, $\bar{\mu}_\theta(n,\theta_0)$, may also be of interest. The latter can be calculated from the time averaged spark distribution, or from the time history of the ensemble mean spark angle if these are available,

$$\bar{\boldsymbol{\mu}}_{\boldsymbol{\theta}}(n,\theta_0) = \boldsymbol{\theta}^T \bar{\mathbf{P}}_n(\boldsymbol{\theta}) = \frac{1}{n}\sum_{j=1}^{n}\boldsymbol{\mu}_j(\boldsymbol{\theta}) \tag{25}$$

A more computationally efficient approach, however is to compute the time-averaged mean directly. To this end, let $S(n,\theta_i)$ be the expected total sum of closed loop spark advance angles, starting at initial spark angle θ_i. If we have a knock event in the first cycle, then the conditional expected sum of spark angles in the first n+1 cycles is the current angle plus the expected sum in the first n cycles starting at $\theta_{i-m_2'}$. If there was no knock event in the first cycle, then the conditional sum over the first n+1 cycles is the current angle plus the expected sum in the first n cycles, only this time starting at $\theta_{i+m_1'}$. The value of the expected total summation may therefore be expressed recursively as,

$$S(n+1,\theta_i) = p'(\theta_i)\, S(n,\theta_{i-m_2'}) + (1-p'(\theta_i))\, S(n,\theta_{i+m_1'}) + \theta_i \tag{26}$$

where the condition $S(0,\theta_i) = 0$ for all θ_i is used to start the recursion. A similar expression for the desired time averaged mean spark angle, $\bar{\mu}_\theta(n,\theta_i)$ then follows directly,

$$\bar{\mu}_\theta(n+1,\theta_i) = \frac{n}{(n+1)}\left(p'(\theta_i)\, \bar{\mu}_\theta(n,\theta_{i-m_2'}) + (1-p'(\theta_i))\, \bar{\mu}_\theta(n,\theta_{i+m_1'})\right) + \frac{1}{(n+1)}\theta_i \tag{27}$$

In order to iterate (27), it is convenient to compute $\bar{\mu}_\theta(n,\theta_i)$ simultaneously for all θ_i according to,

$$\bar{\boldsymbol{\mu}}_{\boldsymbol{\theta}}(n+1,\boldsymbol{\theta}) = \frac{n}{(n+1)}\mathbf{M}\,\bar{\boldsymbol{\mu}}_{\boldsymbol{\theta}}(n,\boldsymbol{\theta}) + \frac{1}{(n+1)}\boldsymbol{\theta} \tag{28}$$

where $\bar{\boldsymbol{\mu}}_{\boldsymbol{\theta}}(n,\boldsymbol{\theta})$ is a column vector whose (i+1)*th* element is $\bar{\mu}_\theta(n,\theta_i)$. The result, for a variety of different initial spark angles, is shown in Fig. 10. As might be expected, the responses appear slightly slower, and are smoother than the corresponding ensemble-averaged results (compare Fig. 8), due to the low-pass filtering effect of the time-averaging process. The traces also converge and settle quite rapidly at the steady state ensemble mean value, (in contrast to the ensemble averaged transient response which exhibits a persistent periodic oscillation as discussed above). Indeed the final value of the time-averaged mean spark angle is easily obtained from (28) as the solution to

$$\lim_{n\to\infty}\,(\mathbf{M}-\mathbf{I})\,\bar{\boldsymbol{\mu}}_{\boldsymbol{\theta}}(n,\boldsymbol{\theta}) = 0 \tag{29}$$

as n tends to infinity. Note that the traces converge quite rapidly to the steady state ensemble mean value, and indeed

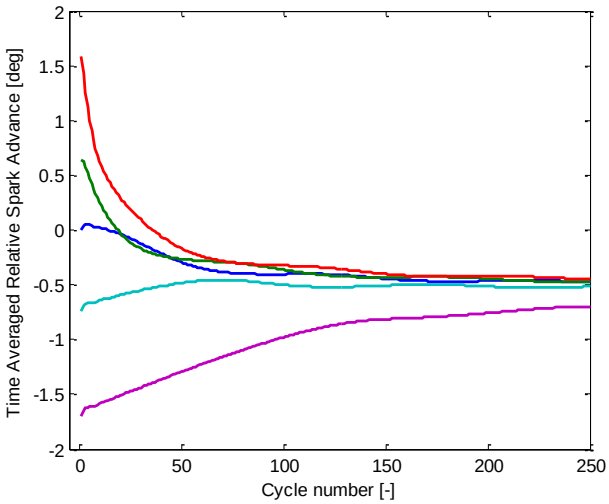

Fig. 10: Transient response of the time-averaged mean spark advance from different initial conditions.

4.3 *Finding the expected spark advance transient response time.*

The time histories of the mean spark advance or instantaneous knock probability, such as those shown in Figs. 8,9, provide a useful insight into the transient performance of the controller, but it would be useful to quantify this in some way. One possibility is to define $T(\theta_{targ \pm tol}, \theta_i)$ as the expected time or number of cycles needed for the controller to return the spark angle from some initial disturbance value, θ_i, to within some specified tolerance of a 'target' spark condition, θ_{targ}. Note that the value of $T(\theta_{targ \pm tol}, \theta_i)$ (the expected response time of all traces) will be slightly different from the time taken for the ensemble trace to reach the same specified target condition. One choice for θ_{targ} might be the desired BL condition, but as observed in Section 3, it is often the case that the steady state value is retarded relative to θ_{BL}. This would bias the response times, making the apparent retard response of the controller faster, and the apparent advance response slower. A more appropriate metric is therefore to measure the expected time $T(\theta_{ss \pm tol}, \theta_i)$ taken for the spark angle response to fall within some defined tolerance of the steady state spark angle value.

Whatever 'target' spark angle θ_{targ} is chosen, it would be useful to be able to compute the corresponding response time metric $T(\theta_{targ}, \theta_i)$ directly. Clearly, if the spark advance is already at the target, the response time $T(\theta_{targ}, \theta_{targ}) = 0$. For any other θ_i, the response time is at least one cycle (corresponding to the first step), plus the response time measured from the new spark angle at the next step. This new response time is $T(\theta_{targ}, \theta_{i-m_2'})$ if the controller responded to a knock event, or $T(\theta_{targ}, \theta_{i+m_1'})$ if no knock event occurred. The desired response time can therefore be expressed as,

$$T(\theta_{targ}, \theta_i) = 1 + p'(\theta_i) T(\theta_{targ}, \theta_{i-m_2'}) + (1 - p'(\theta_i)) T(\theta_{targ}, \theta_{i+m_1'}) \quad (30)$$

where the $p'(\theta_i)$ term is dropped if θ_i and $\theta_{i-m_2'}$ are on different sides of θ_{targ}, and the $(1 - p'(\theta_i))$ term is dropped if θ_i and $\theta_{i-m_2'}$ are on different sides of θ_{targ}.

In order to solve for $T(\theta_{targ},\theta_i)$, it is necessary to write (30) for each possible θ_i, resulting in a set of linear equations that can be written in matrix form as,

$$\mathbf{T}(\theta_{targ},\boldsymbol{\theta}) = \mathbf{M}^{*}\ \mathbf{T}(\theta_{targ},\boldsymbol{\theta}) + \mathbf{C} \tag{31}$$

where $\mathbf{T}(\theta_{targ}, \boldsymbol{\theta})$ is a column vector whose $(i+1)$th element is $T(\theta_{targ}, \theta_i)$, and $\mathbf{C}$ is an identically sized vector containing all ones apart from the element $(targ+1)$ which is zero. The matrix $\mathbf{M}^{*}$ is defined similarly to (15), only eliminating those terms that would result in crossing the θ_{targ} threshold:

$$\begin{cases} \mathbf{M}^{*}_{i,i-m_2'} = p(\theta_i) & \forall\ i \mid (1 \le i \le i_{\max}) \text{ AND } [(i < targ) \text{ OR } (i - m_2' > targ)] \\ \mathbf{M}^{*}_{i,i+m_1'} = \left(1 - p(\theta_i)\right) & \forall\ i \mid (1 \le i \le i_{\max}) \text{ AND } [(i > targ) \text{ OR } (i + m_1' < targ)] \end{cases} \tag{32}$$

Assuming (31) has a solution, the desired response times $T(\theta_{targ}, \theta_i)$ for the spark advance to reach or cross the θ_{targ} value, for any initial spark angle θ_i, can be found according to,

$$\mathbf{T}(\theta_{targ},\boldsymbol{\theta}) = -\left(\mathbf{M}^{*} - \mathbf{I}\right)^{-1}\mathbf{C} \tag{33}$$

Evaluating (33) for θ_{targ} = -0.53°, (which is the mean steady state spark angle obtained from (17), (23)), gives the results shown in Fig. 11. If the initial spark is retarded relative to the steady state condition, the response time is comparatively slow (due to the small advance gain) and, as might be expected, the number of cycles required to reach steady state increases approximately linearly with the difference θ_{ss}-θ_0. If the initial spark is advanced relative to the steady state condition, however, the response time characteristic is quite different. The time is shortest when θ_0-θ_{ss} is slightly less than some integer multiple of the retard gain since if θ_0-θ_{ss} = 1°, for example, then if a knock event occurs, the steady state spark angle can be reached in a single step. It is interesting to note that the response time is significantly longer when θ_0-θ_{ss} is small. In this case, although the steady state spark angle can be reached in a single retard step, the probability of a knock event occurring is much smaller, and the spark timing is likely to be advanced away from the steady state spark angle. The response time is also significantly longer if θ_0-θ_{ss} is slightly more than some integer multiple of the retard gain, since knock events which occur with higher probability will retard the spark into the 'small' θ_i-θ_{ss} region, where as discussed above, the response will be slow.

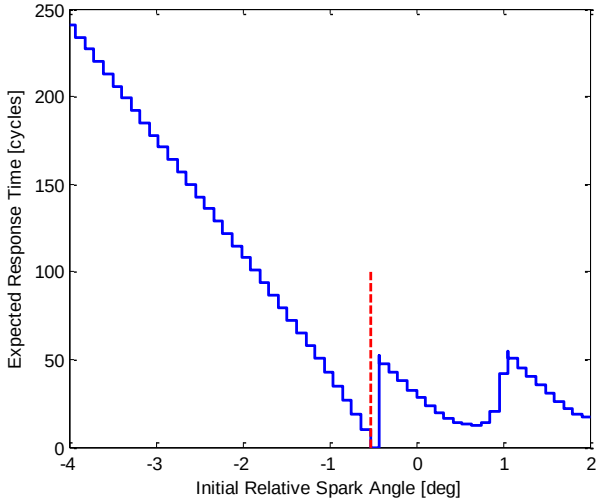

Fig. 11: Expected closed loop response time in cycles as a function of initial relative spark angle disturbance

4.2 *Finding the distribution of the number of knock events in the first n cycles.*
Although the closed loop response time of the controller provides a useful metric for controller performance, it could be argued that the speed of the response is less important than the number of knock events that occur during this transient - or during any specified number of cycles relative to some given initial condition. This number belongs to a distribution which depends both on the initial spark advance, and on the closed loop knock control law. To compute the distribution, define $P_n(k,\theta_i)$ to be the probability of getting exactly k knock events in the first n cycles starting at θ_i. Clearly zero knock events are always obtained in the first zero cycles, so $P_0(0,\theta_i) = 1$ for all θ_i. More generally, however, in order to have k knock events in the first $n+1$ cycles, there must be either a) a knock event in the first cycle, followed by k -1 knock events in the next n cycles or b) no knock event in the first cycle, followed by k knock events in the next n cycles. The desired distribution of the number of knock events in the first n cycles can therefore be obtained recursively as,

$$P_{n+1}(k,\theta_i) = p'(\theta_i)\,P_n(k-1,\,\theta_{i-m_2'}) \;+\; (1-p'(\theta_i))\;P_n(k,\theta_{i+m_1'}) \tag{34}$$

Inspection of (34) shows that the desired distribution, starting at angle θ_i is dependent on earlier distributions starting at other initial conditions $\theta_{i-m_2'}$, $\theta_{i+m_1'}$. Since these dependencies expand recursively back to n=1, it is easier to compute $P_n(k;\theta_i)$ simultaneously for all θ_i. Equation (34) can therefore be rewritten in matrix form, as,

$$\mathbf{P}_{n+1}(\mathbf{k},\boldsymbol{\theta}) = \;\mathbf{M}^{ret}\;\mathbf{P}_n(\mathbf{k}-1,\boldsymbol{\theta}) \;+\; \mathbf{M}^{adv}\;\mathbf{P}_n(\mathbf{k},\boldsymbol{\theta}) \tag{35}$$

where $\mathbf{P}_n(\mathbf{k},\boldsymbol{\theta})$ is a matrix whose (i+1,k+1)th element is $P_n(k;\theta_i)$, and where matrices $\mathbf{M}^{ret}$, $\mathbf{M}^{adv}$, already defined in (14), encapsulate the relevant transition probabilities. Note that the (i+1)th row of $\mathbf{P}_n(\mathbf{k}, \boldsymbol{\theta})$ gives the entire probability distribution for the number of knock events occurring in the first n cycles, starting from initial condition θ_i. Iterating (35) for n=100 cycles, from an initial condition θ= BL+0.7°, for example, gives the distribution shown in Fig. 12. In this case, starting from an initially advanced condition, it can be seen that there are most commonly 2 knock events in the first 100 cycles, but 1 or 3 knock events can also be observed occasionally.

Only a single knock event would be expected if the controller were operating as desired at the target 1% rate, and the difference is therefore due to the higher knock rate experienced during the transient response of the system.

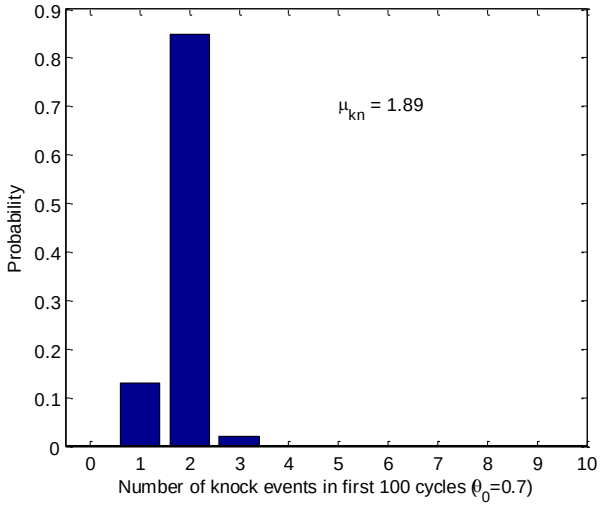

Fig. 12: Distribution of the number of knock events in the first 100 cycles, with initial spark angle θ_0=BL+0.7°

4.3 *Finding the expected number of knock events in the first n cycles*

Although it is possible to compute $\mathbf{P}_n(\mathbf{k},\boldsymbol{\theta})$ for different cycle numbers n, and to observe how the distribution such as that shown in Fig 12 evolves with time, the three-dimensional nature of the results makes them hard to visualize. A simpler approach is plot only the expected number of knock events $\mu_{kn}(n,\theta_i)$ in the first n cycles, starting from initial condition θ_i. If $\mathbf{P}_n(\mathbf{k},\boldsymbol{\theta})$ is already available, the latter is readily computed according to,

$$\mu_{kn}(n,\theta_i) = \sum_{k=0}^{n} P_n(k,\theta_i)\ k \tag{36}$$

It is also possible, however, to obtain $\mu_{kn}(n,\theta_i)$ more directly from a first step analysis. If we have a knock event in the first cycle, then the conditional expected number of knock events in the first $n+1$ cycles is one plus the expected number of knock events in the first n cycles starting at $\theta_{i-m_2'}$. If we have no knock event in the first cycle, then the expected number of knock events in the first $n+1$ cycles is simply the same as the expected number of knock events in the first n cycles starting at $\theta_{i+m_1'}$. The desired expectation can therefore be found recursively according to,

$$\mu_{kn}(n+1,\theta_i) = p'(\theta_i)\left(1+\mu_{kn}(n,\theta_{i-m_2'})\right) + (1-p'(\theta_i))\ \mu_{kn}(n,\theta_{i+m_1'}) \tag{37}$$

where the initial solution is given by $\mu_{kn}(0,\theta_i) = 0$ for all θ_i, since it is not possible to have a knock event when n=0. As before, it is convenient to express (37) in matrix form as,

$$\boldsymbol{\mu}_{\mathbf{kn}}(n+1,\boldsymbol{\theta}) = \mathbf{M}\ \boldsymbol{\mu}_{\mathbf{kn}}(n,\boldsymbol{\theta}) + \mathbf{p}'(\boldsymbol{\theta}) \tag{38}$$

where $\boldsymbol{\mu}_{\mathbf{kn}}(n,\boldsymbol{\theta})$ and $\mathbf{p}'(\boldsymbol{\theta})$ are vectors whose $(i+1)$th elements are $\mu_{kn}(n,\theta_i)$ and $p'(\theta_i)$ respectively. Clearly the number of knock events computed using (38) will increase with time, so it is easier to

assess the results by plotting the excess or deficiency of knock events relative to the expected number if the system were operating at the target knock probability, p. The result, for a variety of different initial spark angles is shown in Fig. 13. A steeply rising trace indicates that the expected number of knock events is rising much more rapidly than the expected target, while a horizontal trace indicates that the expected number of knock events matches the target. As seen from Fig 13, a more advanced initial spark angle causes the number of knock events to increase sharply relative to the expected target during the initial transient, but the response then flattens as the controller compensates for this disturbance. Similarly, a more retarded spark angle causes the expected number of knock events to decrease (relatively slowly) relative to the expected target until the controller compensates for the disturbance, and the response then flattens again. Note also the relationship between Figs. 12 and 13: The expected number of knock events at cycle 100, for initial condition θ_0=BL+0.7° (shown annotated in Fig 13), corresponds to the mean of the distribution shown in Fig 12.

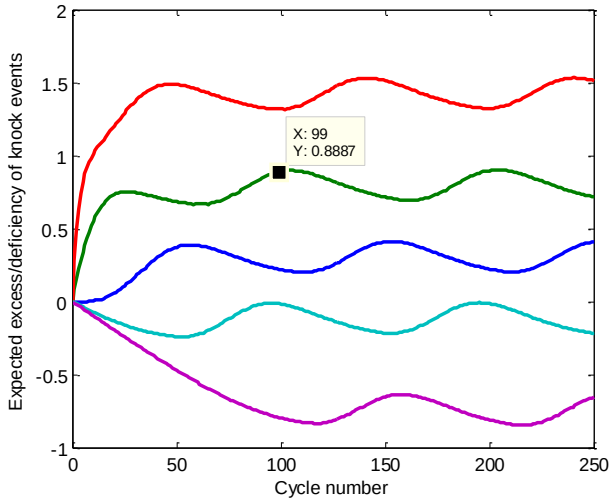

Fig. 13: Expected excess or deficiency of knock events as a function of cycle number for different initial spark angle disturbances θ_0 = {-1.6, -0.7, 0, 0.7, 1.6} degrees respectively

4.4 *Finding the expected number of knock events during the transient response*

The number of knock events occurring during the transient response of the engine provides a useful complement to the response time, $T(\theta_{ss}, \theta_i)$ or $T(\theta_{BL}, \theta_i)$ itself. To this end, define $\mu_{k\theta}(\theta_{targ},\theta_i)$ to be the expected number of knock events until returning to (or passing over) some target spark angle such as $\theta_{targ} = \theta_{ss}$ or $\theta_{targ} = \theta_{BL}$, starting from an initial spark angle, θ_i. Clearly, if θ_i equals θ_{targ}, then we have $\mu_{k\theta}(\theta_{targ},\theta_{targ}) = 0$. For all other values of θ_i, a similar first step analysis as that used to derive (30) yields,

$$\mu_{k\theta}(\theta_{targ},\theta_i) = p'(\theta_i)\left(1+\mu_{k\theta}(\theta_{targ},\theta_{i-m_2'})\right) + (1-p'(\theta_i))\,\mu_{k\theta}(\theta_{targ},\theta_{i+m_1'}) \qquad (39)$$

where, as in (30), the $p'(\theta_i)$ term is dropped if θ_i and $\theta_{i-m_2'}$ are on different sides of θ_{targ}, and the (1- $p'(\theta_i)$) term is dropped if θ_i and $\theta_{i-m_2'}$ are on different sides of θ_{targ}. In matrix form this becomes,

$$\boldsymbol{\mu}_{\mathbf{k\theta}}(\theta_{targ},\boldsymbol{\theta}) = \mathbf{M}^{*}\,\boldsymbol{\mu}_{\mathbf{k\theta}}(\theta_{targ},\boldsymbol{\theta}) + \mathbf{D} \tag{40}$$

where $\mathbf{M}^{*}$ is defined in (32), and where $\mathbf{D}$ is a column vector whose (i+1)th element is $p'(\theta_i)$ except for element ($targ$+1) which is zero. The expected number of knock events to reach (or pass over) θ_{targ}, from every possible initial spark angle θ_i, is then given by,

$$\boldsymbol{\mu}_{\mathbf{k\theta}}(\theta_{targ},\boldsymbol{\theta}) = -\left(\mathbf{M}^{*}-\mathbf{I}\right)^{-1}\mathbf{D} \tag{41}$$

Using (41) to evaluate $\boldsymbol{\mu}_{\mathbf{k\theta}}(\theta_{ss},\boldsymbol{\theta})$ for the example system gives the results presented in Fig. 14. Comparing to Fig. 11 shows that under retarded conditions, although the time taken to reach the steady state increases rapidly with the difference θ_{ss}-θ_i, the low knock probability in this region means that the number of knock events is fairly constant (at around 0.1 events on average), only reducing to zero as the target spark angle is approached. If however, the initial spark is advanced relative to the steady state condition, then at least one knock event is needed to reach θ_{ss} if the initial spark angle is in the range $0<\theta_i - \theta_{ss} < K_{ret}$. If a knock event does not arrive before the spark has been incremented beyond the K_{ret}, boundary, or if the initial spark advance $\theta_i - \theta_{ss}$ was greater than K_{ret}, then at least two knock events are required, and so on. This gives rise to the large step-like characteristic seen in Fig. 14.

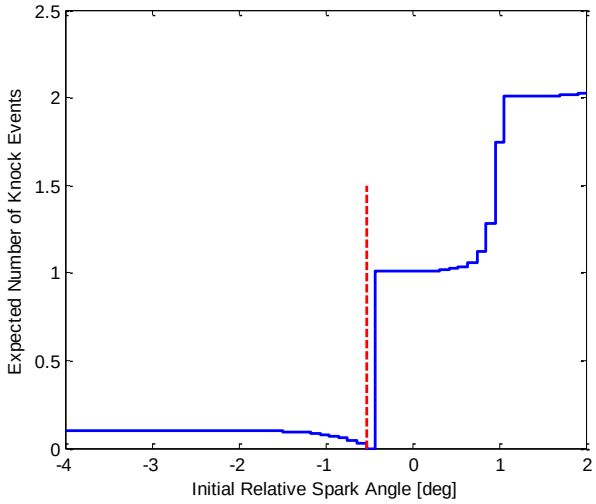

Fig. 14: Expected number of knock events as a function of initial relative spark angle disturbance

5. Conclusions

The performance of knock control systems has previously been assessed largely through either real or simulated closed-loop experiments, but the results of such analysis are heavily dependent on the particular instance of the knock process experienced during the specific test. A different sequence of knock events may result in a very different closed-loop time history, making it hard to obtain repeatable, rigorous metrics for closed-loop controller performance. In this work, a Markov-based stochastic simulation and analysis approach has been extended and new performance metrics derived in order to quantify both the steady state and transient performance of the controller.

The steady state results show the undesirably broad nature of the closed loop spark advance distribution, and the highly skewed nature of the instantaneous knock probability distribution. The transient evolution of these distributions with time / cycle number following some initial disturbance has also been investigated and quantified both in terms of the expected recovery response time, and the expected number of knock events during this period. These results show that the transient performance of the system is nonlinearly dependent on the magnitude of the applied disturbance, further emphasizing the dangers of using a single simulation or a small set of experimental results to assess the controller performance. The stochastic computation methods outlined above, provide a much more rigorous and complete description of closed loop behavior. In future work this tool will be used to investigate how the performance varies with tuning of the controller parameters, and the approach extended to stochastic simulation of more advanced controller strategies.

ACKNOWLEDGEMENTS

This work was supported in part by the Briar Hill Foundation and ExxonMobil, and the data was provided by Ford Motor Company.

REFERENCES

1. Heywood JB. *Internal combustion engines fundamentals*. McGraw–Hill, New York, 1988.
2. Eckert P, Kong S, and Reitz R. Modeling autoignition and engine knock under spark ignition condition. SAE paper 2003–01–0011, 2003.
3. Teraji A, Tsuda T, et al. Development of a three–dimensional knock simulation method incorporating a high–accuracy flame propagation model. *Int J Engine Research* 2005; 6: 73–83.
4. Borg JM and Alkidas AC. On the application of Weibe functions to simulate normal and knocking spark–ignition combustion. *Int J Vehicle Design* 2009; 49: 52–69.
5. Forte C, Corti E, and Bianchu GM. Combined experimental and numerical analysis of knock in spark ignition engines. In: Proceedings of the ASME 2009 Internal Combustion Engine Division Fall Technical Conference, Lucerne, Switzerland, 20 Sep – 24 Sep 2009, pp. 473–488.
6. Peyton Jones JC and Muske KR. A data–base driven in–cycle engine simulator for control, calibration and robustness testing. SAE paper 2008–01–1002, 2008.
7. Schmillen KP and Rechs M. Different methods of knock detection and knock control. SAE paper 910858, 1991.
8. Zhu G, Haskara I, and Winkleman, J. Stochastic limit control and its application to spark limit control using ionization feedback. SAE paper 2005–01–0018, 2005.
9. Sinnerstad, K. *Knock intensity and torque control on an SVC engine*. Master's Thesis, Linköping University, SE, 2003.
10. Naber JD, Blough JR, Frankowski D, et al. Analysis of combustion knock metrics in spark–ignition engines. SAE paper 2006–01–0400, 2006.
11. Wu, G. A real time statistical method for engine detection. SAE paper 2007–01–1507, 2007.
12. Abhijit and Naber JD. Ionization signal response during combustion knock and comparison to cylinder pressure for SI engines. SAE paper 2008–01–0981, 2008.

13. Lonari, Y, Polonowski C, Naber J, et al. Stochastic knock detection model for spark ignition engines. SAE paper 2011–01–1421.
14. Spelina JM, Peyton Jones JC and Frey J. Characterization of knock intensity distributions, Part II: parametric models. *Proc IMechE, Part D: J. Auto Eng*, vol. 227, pp.1650-1660, (2013).
15. Kiencke U and Nielsen L. *Automotive control systems for engine, driveline, and vehicle* (2nd ed.). Springer, New York, 2005.
16. Papoulis, A and Pillai SU. *Probability, random variables and stochastic processes* (4th ed.). McGraw–Hill, New York, 2002.